ACS APPLIED MATERIALS & INTERFACES

Research Article

www.acsami.org

Formation of Shish-Kebabs in Injection-Molded Poly(L-lactic acid) by Application of an Intense Flow Field

Huan Xu,[†] Gan-Ji Zhong,*[,†] Qiang Fu,[†] Jun Lei,[†] Wei Jiang,[‡] Benjamin S. Hsiao,[§] and Zhong-Ming Li*[,†]

[†]College of Polymer Science and Engineering, State Key Laboratory of Polymer Materials Engineering, Sichuan University, Chengdu, 610065, Sichuan, People's Republic of China

[‡]State Key Laboratory of Polymer Physics and Chemistry, Changchun Institute of Applied Chemistry, Chinese Academy of Sciences, Changchun, 130022, People's Republic of China

[§]Department of Chemistry, Stony Brook University, Stony Brook, New York 11794-3400, United States

ABSTRACT: Unlike polyolefins (e.g., isotactic polypropylene), it is still a great challenge to form rich shish-kebabs in biodegradable poly(L-lactic acid) (PLLA) because of its short chain length and semirigid chain backbone. In the present work, a modified injection molding technology, named oscillation shear injection molding, was applied to provide an intense shear flow on PLLA melt in mold cavity, in order to promote shear-induced crystallization of PLLA. Additionally, a small amount of poly(ethylene glycol) (PEG) with flexible chains was introduced for improving the crystallization kinetics. Numerous shish-kebabs of PLLA were achieved in injection-molded PLLA for the first time. High-resolution scanning electronic microscopy and small-angle X-ray scattering showed a structure feature of shish-kebabs with a diameter of around 0.7 μm and a long period of ~20 nm. The wide-angle X-ray diffraction results showed that shish-kebabs had more ordered crystalline structure of α-form. A significant improvement of the mechanical properties was obtained; the tensile strength and modulus increased to 73.7 and 1888 MPa from the initial values of 64.9 and 1684 MPa, respectively, meanwhile the ductility is not deteriorated. Interestingly, when shish-kebabs form in the PLLA/PEG system, a bamboo-like bionic structure comprising a hard skin layer and a soft core develops in injection-molded specimen. This unique structure leads to a great balance of mechanical properties, including substantial increments of 26, 20, and 112% in the tensile strength, modulus, and impact toughness, compared to the control sample. Further exploration will give a rich fundamental understanding in the shear-induced crystallization and morphology manipulation of PLLA, aiming to achieve superior PLLA products.

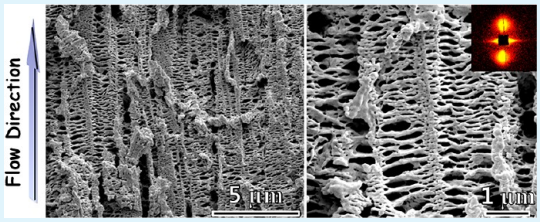

KEYWORDS: *shish-kebabs, poly(L-lactic acid), intense shear flow, polymorphism, bamboo-like structure, performance*

INTRODUCTION

Poly(L-lactic acid) (PLLA) derives from renewable natural sources and can biodegrade to carbon dioxide and water under certain conditions such as the presence of oxygen. PLLA exhibits many advantages compared to other biodegradable polymers, such as relatively low cost, excellent mechanical properties, good processability, and wide range of degradation rates, representing a highly promising and versatile category of environmental friendly materials as well as biomaterials.[1−3] Although PLLA is of great promise in the packaging area, its low resistance to oxygen, carbon dioxide and water, and low ductility, which largely lie in its low crystallinity and semirigid molecular backbone, are still obstacles for wider applications. Meanwhile, pure PLLA usually cannot be accepted for use in bone tissue engineering, which needs ultrahigh strength and elastic modulus to prevent stress-shielding atrophy and weakening of the fixed bone,[4−6] because the spherulites usually formed in PLLA products have low mechanical properties.

A good deal of approaches have been proposed in an endeavor to obtain high-performance PLLA products, including copolymerization, blending, making composites, and self-reinforcement.[6−9] Among these methods, self-reinforcement, exploiting manipulation of crystalline superstructure in drawing or flow fields (i.e., formation of oriented microstructure containing extended polymer chains), never fails to attract peoples' attention due to its efficient enhancement in mechanical properties, great convenience, low density, and environmental benignancy.[9−12] More importantly, compared with other methods, this homogeneous system generated via self-reinforcement technology manifests significant superiority in achieving perfect interfaces between different phases or composite components thanks to pure chemical functionality, which is particularly important in biomedical applications because any additives composed of different chemicals could seriously sacrifice biocompatibility and biodegradability.[9,10,13] The self-reinforcement of PLLA was first attempted by using a solid extrusion technology, a remarkable enhancement of flexural strength (from ~60 MPa for raw sample to ~125 MPa for drawn sample) has been achieved.[14] However, the microstructure responsible for this effect of reinforcement is

Received: September 13, 2012
Accepted: November 16, 2012
Published: November 16, 2012

rarely explored. From the elaborate investigation of other polymer systems such as polyethylene and polypropylene, tremendous self-reinforced effect originates from the shish-kebab superstructure formed in drawing or flow fields, which heterogeneously distributes in bulk as an ideal reinforced element.[15−21] Unfortunately, for PLLA, no one catches a typical picture of PLLA shish-kebab superstructure, especially in common processing, although it is crucial for us to understanding its self-reinforcement effect. Naturally, it stimulates us to obtain PLLA shish-kebabs in final products, thereby concerning with interrelationship between this superstructure and resultant performance.

Some requisite information needs to be born in mind before attempting to obtain PLLA shish-kebab superstructure. Considerable progress since the early 1960s has been made in understanding the flow-induced shish-kebab superstructure mainly based on the shear-induced crystallization of polyethylene and polypropylene in solutions or melts.[19,22−32] Although the molecular understanding of shish nucleation is still controversial,[21,33,34] a large wealth of experimental evidence suggest that multiple critical parameters exist for the formation of shish-kebab superstructure, which may give us more useful guidelines for preparation of PLLA shish-kebabs. For instance, a small amount of high molecular weight chains beyond a critical molecular weight (M^*) are usually considered to be efficient to form precursors for shish nucleation since long chains need long time to disengage once they are stretched by a flow field.[35−38] Besides M^*, there could exist some critical flow parameters, such as critical shear rate greater than Rouse time,[30] critical strain,[39] and critical specific work of flow.[29] As a generalization, the formation of shish-kebab superstructure needs high enough strain and shear rate as well as appropriate molecular weight and its distribution, which are crucial for the formation of stable nuclei after the orientation and alignment of chains rather than relaxation and disengagement.

Unlike polyolefins, few research concerns on flow-induced superstructure of PLLA, which comes from the family of aliphatic polyesters that have relatively rigid molecular backbone and low molecular weight.[40,41] Although these polymers always outperform polyolefins, e.g., tensile strength, stiffness, abrasion resistance, and dimensional stability, polyolefins with flexible chains and high steric regularity are usually used for the intensive investigations of shish-kebab superstructure because the chain characters lead to a favorable crystallization kinetics, and it is relatively easy to stretch and orient chains to obtain this superstructure. On the other hand, it is more difficult to form a shish-kebab superstructure for the polymers with relatively rigid backbone.[41] For instance, we proved only a weak orientation of poly(phenylene sulfide) crystals induced by shear field, and thus only a small amount of cylindrical crystalline superstructure, regarding as overgrowth of shish-kebab superstructure, formed under a high shear rate or a long shear duration.[40] For PLLA, our previous work based on polarized optical microscopy has shown that the crystallization behavior of PLLA under shear flow depends on the shear rate and crystallization temperature, and the growth of cylindrical crystalline structure occurs only sporadically.[42] Weak shear flow that is not able to stretch and orient PLLA chains to some critical extent, and the absence of fast cooling to freeze and stabilize these shish precursors, may be responsible for the limited progress in preceding investigations. The existing study on PLLA provides a limited insight into its shear-induced shish-kebab superstructure, critical prerequisites for its formation, as well as its contribution to properties. Currently, achieving plenty of PLLA shish-kebab superstructures during factual processing remains a huge challenge, although it is of prime interest in view of tailoring crystalline morphology and thus controlling macroscopic properties of PLLA products.

In this paper, taking note of the success in attaining shish-kebab superstructure of polyolefins,[43,44] we attempt to introduce sufficiently strong shear flow into PLLA melt during injection molding, not only in order to stretch and orient PLLA molecules but also to suppress the disengagement and relaxation of these oriented chains (segments). To obtain such a shear flow, the oscillation shear injection molding (OSIM) machine, which has two pistons moved reciprocally at the same frequency during the packing stage, is applied to impose high shear flow on molten PLLA in the cavity of mold.[44−46] Meanwhile, a small amount of poly(ethylene glycol) (PEG) with low molecular weight, which is an effective plasticizer and miscible with amorphous PLLA, is added in order to enhance the chain mobility and crystallization kinetics of PLLA.[47,48] The results clearly show that numerous shish-kebabs form in injection-molded PLLA parts by strong shear flow. Besides morphological feature of shish-kebab superstructure in the injection-molded PLLA, the present work also explores the relationship between this superstructure and mechanical properties preliminarily.

EXPERIMENTAL SECTION

Materials. Commercially available PLLA comprising around 2% D-LA (trade name 4032D) was manufactured by NatureWorks (USA), its weight-average molecular weight and number-average molecular weight were 2.23×10^5 and 1.06×10^5 g/mol, respectively. PEG (trade name Carbowax) with a nominal weight-average molecular weight of 3350 g/mol was obtained from Dow Chemical Company (USA).

Sample Preparation. To avoid the degradation due to hydrolysis and prevent the formation of voids during processing, PLLA and PEG were dried at 100 and 45 °C under vacuum overnight before extrusion or injection molding, respectively. Blending PLLA and PEG was carried out in a corotating twin screw extruder (Nanjing Rubber & Plastics Machinery Plant Co. Ltd., China) with a ratio of screw length to its diameter (L/D) of 40. Temperatures in seven zones were set at 40, 60, 130, 150, 170, 170, and 165 °C from feed section to metering section, respectively, and the screw speed was held constantly at 100 rpm. PEG content was fixed at 5 wt %, such a low level can ensure a good miscibility with amorphous phase of PLLA, avoiding migration from the PLLA matrix.[48] The extruded pellets after drying were injection molded into standard double-bone test samples, the barrel temperature profiles were set at 130, 160, 180, 185, and 180 °C from hopper to nozzle, respectively. During packing stage of injection molding process, a controlled shear flow is continuously imposed on the melt by using OSIM technology, which has two hydraulically actuated pistons that move reciprocally at the same frequency of 0.3 Hz and the pressure of 15 MPa, and the shear flow does not cease until the gate of the mold solidifies. The cycle time of the sample preparation by OSIM and conventional injection molding (CIM) was fixed at about 3 min in this study. It should be noticeable that the control samples of neat PLLA and plasticized PLLA (i.e., PLLA/PEG blend) subjected to the same thermal conditions were also prepared (i.e., CIM without oscillation shear flow). Detailed information of the OSIM machine is available in our previous work.[44,45] For the sake of briefness, the resultant injection-molded parts with different processing methods will be referred to through the paper as OSIM PLLA, CIM PLLA, OSIM PLLA/PEG, and CIM PLLA/PEG, respectively. For instance, OSIM PLLA/PEG stands for plasticized PLLA prepared by OSIM, whereas CIM PLLA represents pure PLLA molded by CIM.

Scanning Electronic Microscopy (SEM). A skin-core morphology with different structure at both molecular and supermolecular level

along the thickness of injection-molded bars is expected due to the existence of an inhomogeneous shear flow field (and temperature) from the skin to the core of the bars.[45] Therefore, in order to investigate the details, the crystalline morphology was needed to be checked from outer layer to core layer orderly. Herein we define the four regions that are 50−400, 400−800, 800−1200, and 1200−2000 μm far from the surface as subskin layer, oriented layer, intermediate layer and core layer, respectively, and the subskin, oriented, and intermediate layers are sometimes called as the outer layer for briefness in the context. To observe this layered structure, a small block was cut from the injection-molded part first, then the block was placed in liquid nitrogen for 0.5 h, finally the block was cryogenically fractured along the midcourt line in the flow direction. The smooth fracture surface was etched by a water−methanol (1:2 by volume) mixture solution containing 0.025 mol/L of sodium hydroxide for 14 h at 15 °C, subsequently the etched surface was cleaned by using distilled water and ultrasonication. A field-emission SEM (Inspect F, FEI, Finland) was utilized to investigate the crystalline morphology of the etched samples layer by layer, which were sputter-coated with gold before observations, and the accelerated voltage was held at 5 kV.

Microbeam Wide-Angle X-ray Diffraction (WAXD). A scanning microbeam WAXD experiment was employed to determine orientation, crystalline morphology, and distribution along the thickness of injection-molded PLLA and PLLA/PEG at the beamline BL15U1 of Shanghai Synchrotron Radiation Facility (SSRF, Shanghai, China). To obtain a discernible X-ray scattering intensity, a piece of slice with a width of 4 mm and a thickness of 1 mm was carefully machined from the tensile bar, as shown in Figure 1. The direction

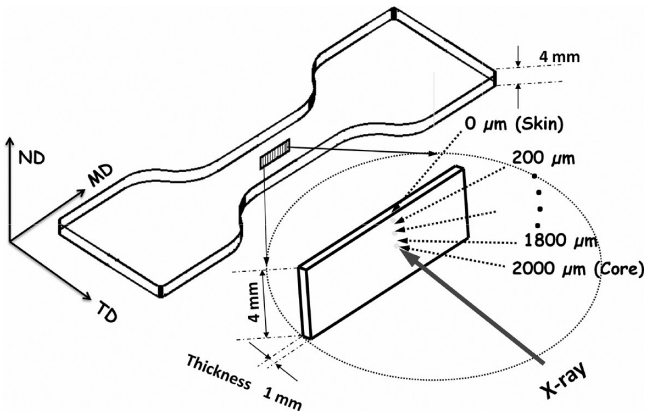

Figure 1. Schematic of sampling method for X-ray diffraction and scattering measurements. Key: MD, the molding direction; TD, the transverse direction; ND, the direction normal to the MD-TD plane.

normal to the MD-TD plane is defined as ND, which is perpendicular to the X-ray beam. We scanned a sample with the X-ray beam from an edge to the core of the sample down from the MD-ND surface with a step of 200 μm as shown in Figure 1. The monochromated X-ray beam with a wavelength of 0.124 nm was focused to an area of 3 × 2.7 μm^2 (length × width), and the distance from sample to detector was 185 mm. Then the 2D-WAXD images were collected with an X-ray CCD detector (model SX165, Rayonix Co. Ltd., USA). Additionally, the WAXD intensity profiles for each 2θ were obtained by integration in the azimuthal angular range of a whole circle (0−360°) from the sample patterns employing the Fit2D package, while background scattering was subtracted from the sample patterns. The intensity profiles were further treated using the Origin 7.5 software, assuming Gaussian profiles for the amorphous halo and all crystalline peaks, and the crystallinity was determined by the ratio of the area under the resolved Gaussian crystalline peaks to the total area under the unresolved diffraction curve.[44]

Small-Angle X-ray Scattering (SAXS). SAXS measurements were performed at the beamline BL16B1 of Shanghai Synchrotron Radiation Facility (SSRF, Shanghai, China) to examine the super-structure structure PLLA in skin layer of injection-molded parts, sample preparation was the same as that of WAXD shown in Figure 1. The SAXS images were collected with an X-ray CCD detector (Model Mar165, a resolution of 2048 × 2048 pixels). The monochromated X-ray beam operated at a wavelength of 0.124 nm with a beam size of 80 × 80 μm^2 (length × width), and the sample-to-detector distance was held at 1900 mm. The radically integrated intensities $I(q)$ ($q = 4\pi\sin\theta/\lambda$) are obtained for integration in the azimuthal angular range of a whole circle, where 2θ is the scattering angle and λ represents the X-ray wavelength.

Mechanical Property Testing. According to ASTM standard D638, the tensile properties were measured at room temperature on an Instron universal test instrument (Model 5576, Instron Instruments, USA) with a crosshead speed of 5 mm/min and a gauge length of 20 mm. The notched Izod impact tests were carried out according to the GB/T 1843−08 standard at room temperature, the dimension of testing specimens were carefully machined to be 50 mm × 6 mm × 4 mm with a V-notch. A minimum of 6 bar for each sample were tested at the same conditions, and the average values were presented with standard deviation.

Dynamic Mechanical Analysis (DMA). To obtain thermomechanical properties and more distinct insights into the interactions of the materials at the molecular level, we conducted DMA. After machining away the both sides of the injection-molded sample, a cubic specimen for DMA measurement with a size of 40 mm ×6 mm ×4 mm (length × width × thickness) was obtained from the middle zone of injection-molded sample. The specimen was carefully placed on the clamp with the MD-TD plane parallel to the horizontal direction and the ND direction upright. The dynamic mechanical properties were measured on a DMA Q800 (TA Instruments, USA) in a multi-frequency strain mode with a dual cantilever clamp (the ASTM standard D4065). And the apparatus was operated with a frequency of 1 Hz, over a temperature range of 20 to 150 °C at a heating rate of 3 °C/min.

RESULTS AND DISCUSSION

Morphological Observation of Shish-Kebabs in Injection-Molded PLLA. The high-resolution SEM observations are first performed to visually exam whether the shish-kebab superstructure is formed in OSIM samples. Figures 2 and 3 show the crystalline morphology and its distribution in

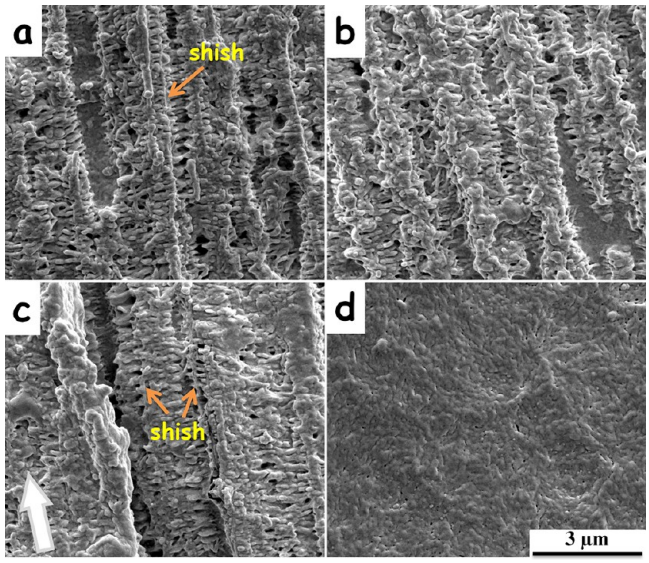

Figure 2. SEM micrographs of different regions of pure PLLA molded via OSIM: (a) subskin layer; (b) oriented layer; (c) intermediate layer; (d) core layer. The big white arrow refers to flow direction, and the magnification factor is held constant.

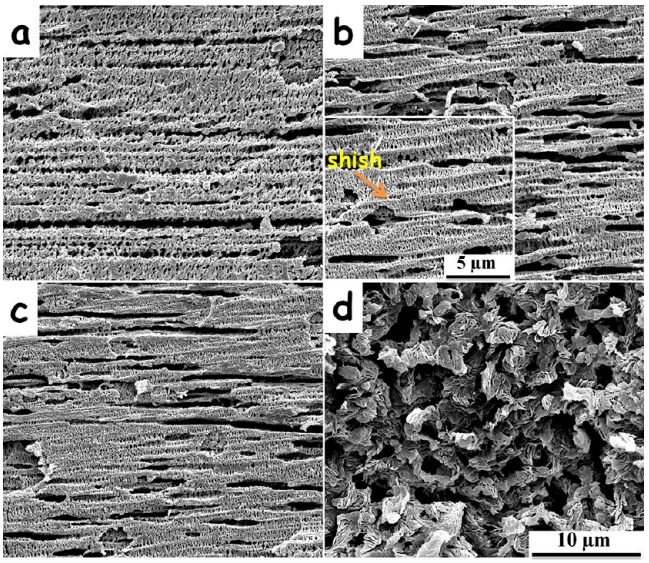

Figure 3. SEM micrographs of different regions of PLLA/PEG molded via OSIM: (a) subskin layer; (b) oriented layer, the inset in higher resolution clearly shows the existing shish; (c) intermediate layer; (d) core layer. The flow direction is horizontal, and the magnification factor is held constantly for a–d except for the inset of b.

injection-molded PLLA and PLLA/PEG samples through OSIM technology. In the OSIM PLLA sample (Figure 2a–c), plenty of cylindrical crystalline entities parallel to each other are observed in the subskin, oriented and intermediate layers (i.e., the outer layer, 50–1200 μm deep from the surface), in which an assembly of closely spaced lamellae grows perpendicularly to the flow direction. This architecture is quite similar to the typical feature of shish-kebab superstructure commonly observed in other orientation-induced semicrystalline polymers like polyethylene and polypropylene.[26,43,49,50] It is tentatively believed that the shish-kebab superstructure of PLLA is, for the first time, formed in injection-molded PLLA sample with the aid of a strong shear flow. These clear high-resolution pictures permit careful measurements of the diameter of the shish-kebabs, which is 1.1 ± 0.2 μm in the subskin layer and decreases gradually to 0.7 ± 0.1 μm and 0.6 ± 0.1 μm for the oriented and intermediate layer, respectively. The moderate fall in the values of shish-kebab diameter from skin to core reflects the effective role of shear flow in facilitating the formation of shish-kebabs, resulting from the oriented chain segments developed in advance subjected to more intense shear flow. As PEG is introduced to PLLA, i.e., the OSIM PLLA/PEG sample (Figure 3a–c), the shish-kebab superstructure is also formed in the outer layer like the case of the OSIM PLLA sample. As shown in Figure 3a–c, compared to that of OSIM PLLA (about 0.7 μm), the diameter of shish-kebabs in cylindrical superstructure dramatically increases to 1.5–1.9 μm for OSIM PLLA/PEG sample, achieving 1.6 ± 0.2, 1.7 ± 0.3, and 1.5 ± 0.3 μm in the subskin, oriented, and intermediate layer, respectively. No obvious variation in the shish-kebab diameter with different depths of injection-molded parts is observed, which indicates that PEG can boost the growth of shish-kebabs and suppresses the hierarchical structure. It implies that PEG may decrease the density of shish, and thus significantly enlarge the diameter of shish-kebab. Note that after addition of PEG, a better contrast of SEM micrographs exists, because PEG is miscible with PLLA amorphous region, when the PEG is dissolved into water during etching process, a leftover of looser amorphous PLLA can be etched away more easily.[48] Furthermore, it is hard to see crystalline superstructure in the core layer of the OSIM PLLA sample as illustrated in Figure 2d, and Figure 3d reveals only typical spherulites in the same layer for the OSIM PLLA/PEG sample. The absence of oriented crystallites in the core region of the two samples is probably derived from the fact that the gate is solidified before the core layer absolutely freezes, hence the sheared PLLA melt still has a longer time for relaxation.

In clear contrast, Figure 4 suggests that only typical spherulites exhibit in both the CIM PLLA and PLLA/PEG

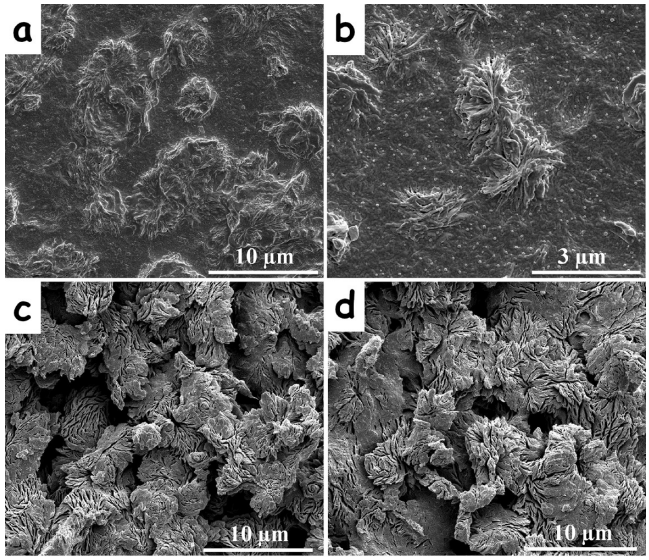

Figure 4. SEM micrographs of CIM samples: (a) outer layer of pure PLLA; (b) core layer of pure PLLA; (c) outer layer of PLLA/PEG; (d) core layer of PLLA/PEG. Two typical regions are selected for comparison.

samples. For the CIM PLLA sample, it is well-established that shear flow will accelerate crystallization due to reduced energy barrier for nucleation.[31] Herein, although relatively high shear rate also exists near the wall of cavity,[45] the strength of shear flow and the duration of shear time generated by CIM are actually unable to be on a par with that of OSIM. Consequently, point-like nuclei tend to form in the outer layer of CIM PLLA sample, instead of long, oriented row-nuclei (shish), and finally develop into spherulites. Images a and b in Figure 4 show that the morphology of spherulites varies along the thickness of the sample. More compact spherulites disperse uniformly in the outer layer with the diameter ranging from 3 to 10 μm, whereas the amount and diameter of spherulites sporadically distributed in the core layer decrease substantially, which evidently infers that the crystallization kinetics of PLLA during injection molding is highly sensitive to shear flow gradient along the thickness, leading to less and smaller spherulites existing in the core layer compared to those in the outer layer. For CIM PLLA sample containing PEG, images c and d in Figure 4 show that the density of PLLA spherulites increases remarkably, and these spherulites have a narrow diameter distribution ranging from 4 to 7 μm, inferring that PEG can act as an effective crystallization accelerator via enhancing chain mobility of PLLA.[51,52] There is no obvious difference in the density and size of spherulites in the outer and

core layers of CIM PLLA/PEG, which further implies that the effect of PEG on crystallization of PLLA prevails over the effect of shear rate gradient during conventional injection molding. In summary, during CIM processing, PLLA melt just develops into spherulitic texture, instead of shish-kebab superstructure. Only when the shear flow is strong enough and the duration is sufficiently long can a transition of spherulite to shish-kebab superstructure happen, as taken place during OSIM.

SAXS measurement was further performed to gain more convincing evidence for formation of shish-kebab superstructure. The representative SAXS patterns are depicted in Figure 5. Images b and d in Figure 5 clearly reveal two sharp

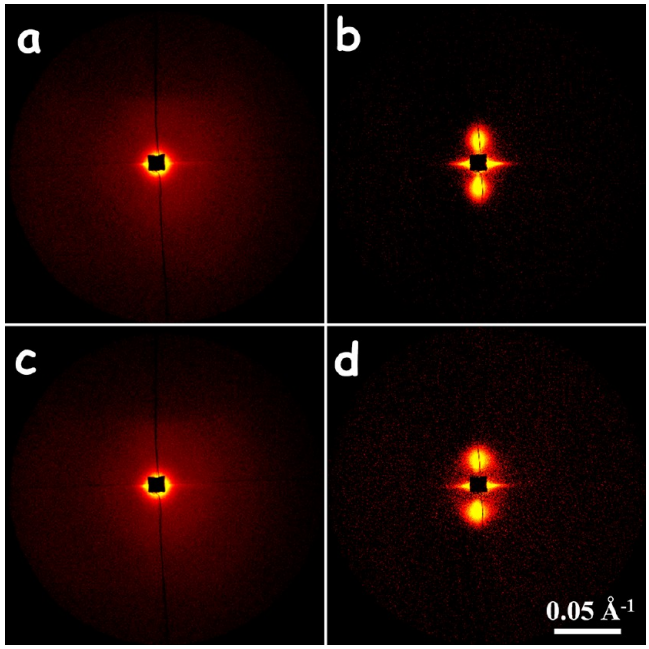

Figure 5. Typical SAXS images measured in subskin layer of (a) CIM PLLA, (b) OSIM PLLA, (c) CIM PLLA/PEG, and (d) OSIM PLLA/PEG. The q-scale bar is inserted.

triangular streaks in the equatorial direction and two bulb-shape lobes in the meridional direction, which are regarded as a typical reflection of shish-kebab superstructure.[24,37] Therefore, combining the SEM observations with the SAXS patterns, we are now confident to confirm the original discovery of PLLA shish-kebab superstructure in injection-molded PLLA samples. In previous work, flow-induced crystallization of PLLA was usually investigated by polarized optical microscopy with a shear hot stage. Only a very small amount of "shish-like" microstructure on the hundreds of micrometer scale was observed under isothermal and nonisothermal crystallization.[41,42,53] It is hard to give a detailed formation of shish structure on nanoscale. Only a preliminary conjecture on the orientations of the columnar structure or on their dimensional information can be made in those studies due to the enlargement limitation. OSIM technique can manipulate the structure development through an in-mold shearing action, conferring on macroscopic shears to the solidifying PLLA melt. Notwithstanding PLLA chains are somewhat short and semirigid,[41] a strong enough shear flow provided by OSIM processing, which outperforms a hot stage coupled with shear cell in providing high shear rate (over 200 s^{-1}) and sufficient shear time (up to ca. 3 min),[44] can still stretch and orient PLLA chains for stable nucleation and growth of shish. Afterward the coiled, entangled chains in the vicinity of the formed shish have the chance to extend and settle on the existing nucleus, leading to a kind of longitudinal growth and, finally showing a unique cylindrical morphology of shish-kebab.[30,31,33,37] For the CIM samples, unexpectedly, the SAXS patterns show no scattering reflection as envisaged in Figure 5a, c, although the spherulites can be observed in both PLLA and plasticized PLLA samples. The missing reflection in SAXS patterns probably lies in the random orientation of the lamellae with the large distribution of lamellar distance, i.e., the lamellar structure is not well developed due to the weak shear flow field during CIM processing, resulting in randomly distributed crystalline lamellae. The similar phenomenon was observed during cold crystallization of PLLA with a crystallization temperature below 110 °C.[54,55]

The intrinsic properties of PLLA chains could be attributed to the feature of PLLA shish-kebabs as observed in CIM PLLA (or PLLA/PEG) sample. PLLA chains have a semirigid backbone and relative low molecular weight, which may be difficult to stretch and orient their chains to produce stable precursors and bundles of chain segments in the way like polyolefins. For polyethylene and polypropylene, even a very weak shearing with short duration may stimulate significant response. As an example, long oriented crystallites of isotactic polypropylene (shishes) developed at a extremely low shear rate of 0.5 s^{-1}.[56] Meanwhile, the oriented PLLA chains tend to relax because the shear-induced row-nuclei do not result from a thermodynamic process, which follows the power law decay $t^{-\alpha}$.[57] It is known that the chain rigidity strongly affects this relaxation process, and the exponent varies from 1/2 for flexible chains to 5/4 for stiff ones.[58] That is the reason why PLLA shish-kebab superstructure rarely exists in CIM samples, although shear flow still occurs during CIM processing. In contrast, during OSIM processing, the strong shear flow with long duration plays a dominate role in inducing the formation of shish-kebabs. The strong, continuous shear flow is powerful to orient PLLA chains, resulting in the formation of plenty of shishes. The amount of shishes seems to depend on the depth in injection-molded parts, which is not observed obviously in OSIM polyolefin parts.[43] By a careful comparison on the crystalline morphology among the subskin, oriented, and intermediate layers, Figure 2 suggest that the amount of shishes decreases and the diameter of the cylindrical superstructure slightly declines along the depth (from 50 to 1200 μm). These results verify again that the relaxation of PLLA shish should be faster than that of flexible polymers such as polypropylene, since the cooling rate decreases gradually along the depth of injection-molded parts. In addition, as PEG is added into PLLA, because of its short chains and excellent miscibility with PLLA chains,[48] it effectively enhances mobility of PLLA molecules. Our results show that increased mobility improves the crystallization kinetics of shish-kebab superstructure (see Figures 2 and 3), leading to longer kebabs because coiled, entangled chains around the shish are apt to fold into lamellae constituting kebabs in an energetically favorable manner.

Figure 6 further shows the SAXS intensity profiles of the four specimens, in order to investigate the lamellar structure in PLLA shish-kebab superstructure quantitatively. The long period between the adjacent kebabs is calculated using the Bragg equation, $L = 2\pi/q^*$, here L is long period, and q^* represents the peak position in the scattering curves.

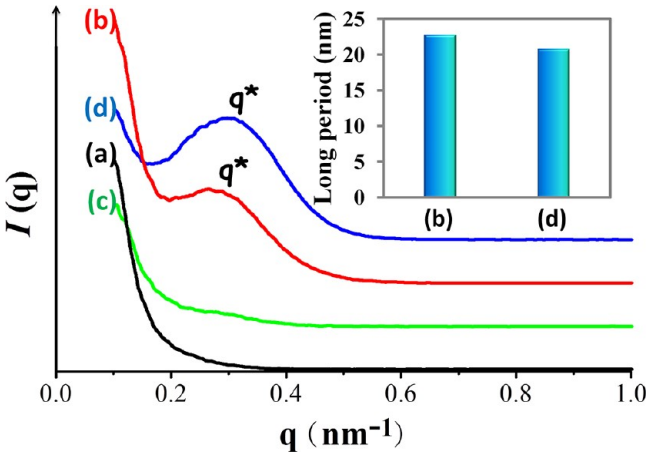

Figure 6. SAXS intensity profiles of (a) CIM PLLA, (b) OSIM PLLA, (c) CIM PLLA/PEG, and (d) OSIM PLLA/PEG. The inset presents the long period of b and d.

Apparently, the OSIM specimens containing shish-kebabs have a maxima around q = 0.3 nm^{-1} in the curves, suggesting a regular aligned lamellar structure with cylindrical symmetry in the PLLA shish-kebab superstructure. In addition, the peak widths at half height for curves b and d were 0.202 and 0.206 nm^{-1}, respectively, which demonstrates that the oriented lamellae of OSIM PLLA and OSIM PLLA/PEG present almost the same uniformity in the distribution of the lamellar periodic distance. Furthermore, we note that the long period of OSIM PLLA sample is 22.8 nm, but it falls to 20.8 nm for OSIM PLLA/PEG. The reduction of 2 nm in long period is probably a result of formation of more compact kebabs, and the accelerated crystallization kinetics of PLLA due to the addition of PEG should also be taken into account.[59] As for the CIM PLLA/PEG sample, the SAXS profile shows a very week broad peak at q = 0.276 nm^{-1}. It is likely attributed to the average spacing of lamella distance with a quite wide distance distribution for the randomly nonoriented lamella morphology in CIM PLLA/PEG.

Molecular Orientation and Crystalline Structure in Injection-Molded PLLA with Shish-Kebabs. Injection-molded semicrystalline polymers generally exhibit spatially inhomogeneous structure (i.e., skin-core structure) especially along the thickness direction because of the existence of flow (or/and thermal) gradient.[60,61] To reveal specific structural information on shish-kebabs in the injection-molded PLLA from skin to core layer, we utilized the microbeam WAXD. Figure 7 presents representative WAXD patterns of skin layer, intermediate layer, and core layer of injection-molded PLLA and PLLA/PEG samples. Evidently, arclike diffraction patterns emerge in the skin and intermediate layers of both OSIM PLLA sample (see Figure 7b) and OSIM PLLA/PEG sample (see Figure 7d) where the shish-kebab superstructure forms, indicating again that the strong shear provided by OSIM can induce shish-kebabs effectively in the outer layer and high molecular orientation. On the other hand, only extremely weak molecular orientation can be found in the skin and intermediate layers of CIM PLLA sample and CIM PLLA/PEG sample as clearly revealed in panels a and c in Figure 7, respectively. It is thus clear that CIM process is not able to generate strong shear flow, resulting in crystalline structure and amorphous chains with poor orientation. In the core layers, in contrast, a halo amorphous diffraction presents in the CIM PLLA sample

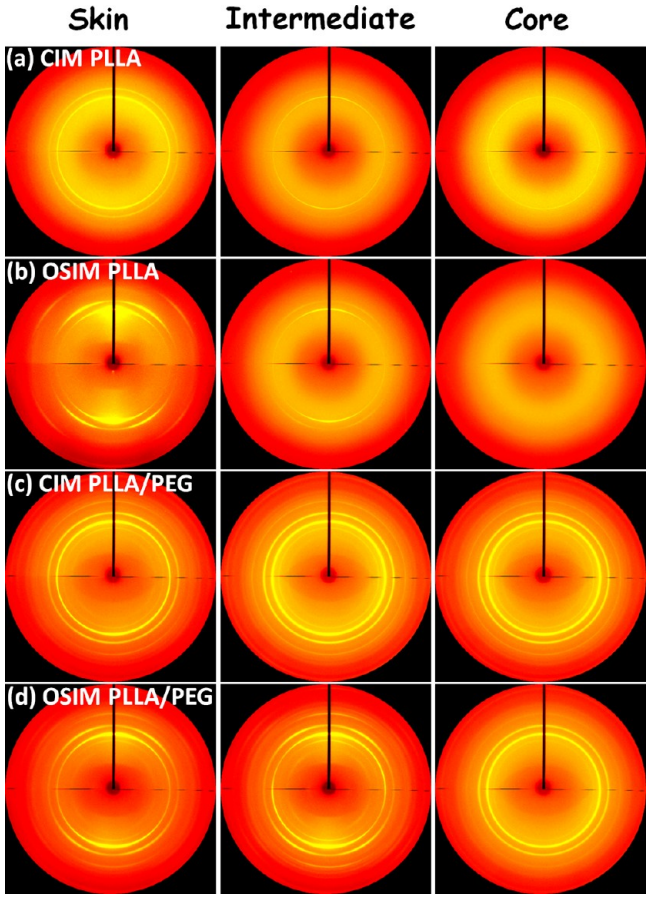

Figure 7. Typically selected WAXD patterns at different regions from skin layer to core layer of injection-molded parts of PLLA and PLLA/PEG.

because of the very low content of spherulites, and a significant enhanced crystallization of PLLA induced by PEG is evidently reflected with a strong homogeneous diffraction reflection. In summary, the WAXD determinations (Figure 7) and SEM observations (Figures 2–4) yield the consistent results on crystalline morphology formed during injection molding.

WAXD intensity profiles are integrated circularly from the corresponding WAXD patterns as shown in Figure 8. The CIM and OSIM PLLA samples have the similar reflection curves (Figure 8a, b), both of which have relatively strong diffraction intensity in the skin and oriented layers and gradually transform to a nearly amorphous halo curve down to the core layer. More interestingly, the polymorphism of PLLA exists in the injection-molded PLLA. Typical reflections of α-form crystal of PLLA can be observed in the subskin and oriented layers of OSIM PLLA (except for the surface), i.e. the typical reflections of α-form crystal at 2θ = 15.1, 16.9, 19.2, and 22.5° corresponding to lattice planes (010), (200)/(110), (203), and (015), respectively.[62] However, in the other layers of OSIM PLLA and all layers of CIM PLLA, no trace of the (010) reflection can be found accompanied by other reflections shifting to a lower value (e.g., lattice plane (200)/(110) shifts from 19.2 to 19.0°), indicating that α'-form crystal with less compact chain conformation and chain packing mode is generated mainly due to slow crystallization kinetics of PLLA and rapid cooling in the processing.[53] When we take the distribution of PLLA crystal modifications and shish-kebab superstructure into consideration together, it appears that the shear effect gives

dx.doi.org/10.1021/am3019756 | ACS Appl. Mater. Interfaces 2012, 4, 6774–6784

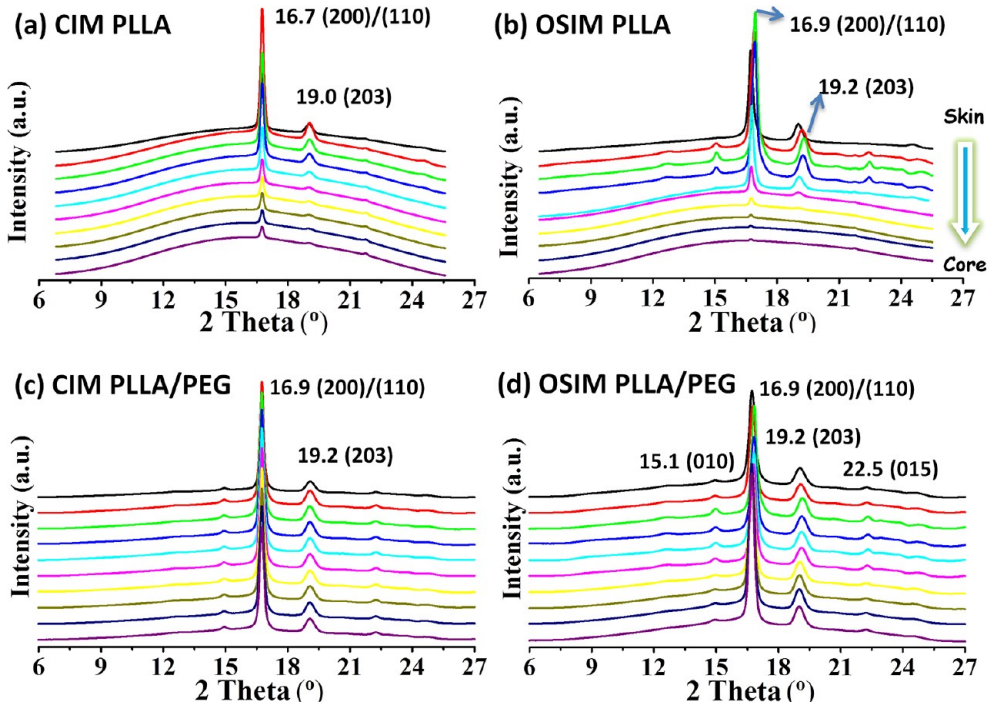

Figure 8. WAXD intensity profiles of injection-molded parts of PLLA and PLLA/PEG from skin layer to core layer, corresponding to the WAXD patterns, every lattice plane is marked around the diffraction peak.

rise to such a compact chain conformation and chain packing mode because of shear-induced oriented molecules and stable precursors, and thus a more ordered crystal structure (α-form) forms in the shish-kebab superstructure. Furthermore, PEG is believed to significantly affect the crystal form when comparing the WAXD results of PLLA/PEG samples with that of pure PLLA. There are four obvious diffraction peaks with stronger diffraction intensity of α-form crystals exhibiting in the areas from skin to core layers of both CIM PLLA/PEG and OSIM PLLA/PEG samples as clearly presented in Figure 8c, d. The crystalline structure of shish-kebabs in the OSIM PLLA/PEG sample is not different from that of spherulites in the CIM PLLA/PEG one, both presenting α-form crystal of PLLA, which could be attributed to the remarkably improved chain mobility by the addition of PEG and consequently easy formation of more ordered chain packing.

The influence of shear flow on the crystallinity and its distribution of injection-molded parts are illustrated in Figure 9. It is generally demonstrated that, under a more intense flow field, the number of parallel chains forming the shish as well as the number of chain segments oriented along the flow direction (so-called precursor) increase significantly.[63] Without doubt, the shear flow provided by OSIM can enhance the crystallinity significantly for pure PLLA. In the outer layer, the crystallinity of OSIM PLLA sample reaches ~22%, which is much higher than that of CIM PLLA one (below 10%). Such a significant improvement of crystallinity in injection molding is rarely reported.[64,65] In general, only crystallization rates can be considerably improved for polyolefins such as polyethylene and polypropylene under shear flow, without remarkable increment of crystallinity. Nevertheless, largely promoted crystallinity is achieved in OSIM PLLA sample, which demonstrates PLLA is highly sensitive to shear flow, and the increase of crystallinity can be reasonably attributed to the formation of rich shish-kebab superstructure. Toward the core layer, the crystallinity of

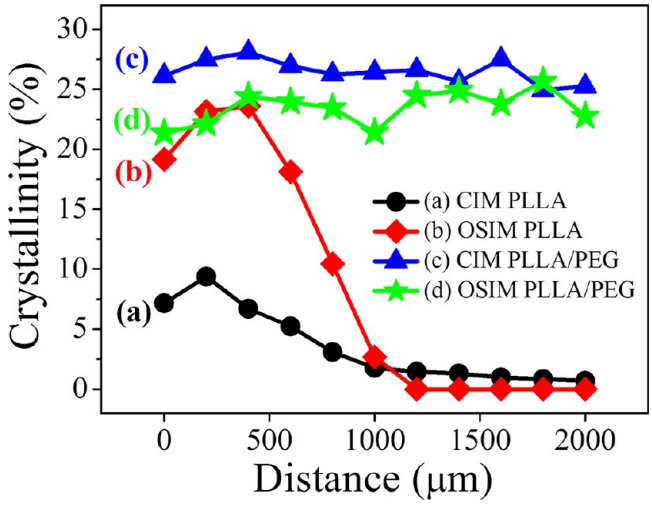

Figure 9. Crystallinity and its distribution of injection-molded parts of PLLA and PLLA/PEG from skin layer to core layer.

both CIM PLLA sample and OSIM PLLA decreases dramatically. This tendency is well in line with the distinct reduced amount of shish-kebab superstructure and spherulites as shown in Figures 2 and 4, respectively. More interestingly, for the PLLA/PEG samples, PEG markedly enhances the crystallization of PLLA especially in core layer, regardless of CIM or OSIM samples, therefore leading to a good maintenance of relatively high crystallinity (ca. 25%) in overall injection-molded parts, such a homogeneous structure could be desirable for fabrication of real products. Moreover, the average crystallinity of OSIM PLLA/PEG is relatively lower (~23%) than that of CIM PLLA/PEG (~26%). Because both PEG and shear flow can accelerate crystallization kinetics of PLLA, a very high crystallization rate is expected and leads to PEG chains have limited time to migrate from PLLA crystalline region into

amorphous during the shear-induced PLLA crystallization. This effect could result in imperfect crystals of PLLA and low crystallinity, although further evidence should be given in the future. On the basis of the previous results, it is worth stressing that when flexible PEG chains is miscible with PLLA, the PEG rather than shear flow plays a more significant role in modifying the crystallization kinetics and crystalline structure of PLLA, whereas shear flow is a dominative factor for manipulating the PLLA superstructure, i.e., transformation from spherulitic texture to shish-kebab superstructure.

Mechanical Performance of Injection-Molded PLLA with Shish-Kebabs. Our next concern is to reveal the influence of shish-kebabs on the bulky performance of PLLA parts. Figure 10 illustrates the typical stress−strain curves of

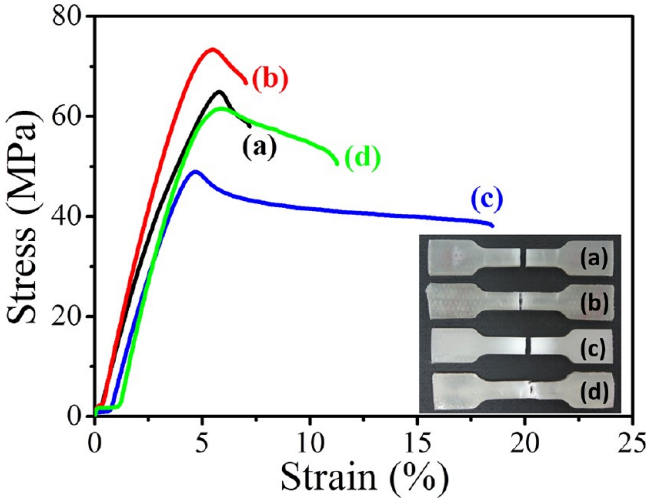

Figure 10. Typical stress−strain curves of (a) CIM PLLA; (b) OSIM PLLA; (c) CIM PLLA/PEG; and (d) OSIM PLLA/PEG. The inset digital photo shows the profiles of the four samples after fracture.

injection-molded PLLA and PLLA/PEG samples. Both CIM PLLA and OSIM PLLA samples perform in a similar tensile behavior, and they basically fracture in a brittle manner with slight plastic deformation. After an addition of PEG, as observed for CIM and OSIM PLLA/PEG samples, the tensile behavior develops into ductile fracture. Considerable strain softening takes place in the samples containing PEG after the yield point, presenting the development of stress whitening as clearly depicted in the inset digital photo of Figure 10. Analysis of the stress−strain curves yields various parameters of tensile mechanical properties, which are summarized in Table 1. Apparently, the CIM PLLA and OSIM PLLA samples experience brittle fracture with low elongations at break of

Table 1. Detailed Mechanical Properties of (a) CIM PLLA; (b) OSIM PLLA; (c) CIM PLLA/PEG; and (d) OSIM PLLA/PEG (results are clarified as average value ± standard deviation after statistical analysis, respectively)

	tensile strength (MPa)	elongation at break (%)	Young's modulus (MPa)	toughness (MJ/m^3)	impact strength (KJ/m^2)
a	64.9 ± 2.6	7.3 ± 0.5	1684 ± 21	3.0	4.5 ± 0.3
b	73.7 ± 3.1	7.1 ± 0.7	1888 ± 33	3.4	4.2 ± 0.4
c	48.9 ± 2.0	18.7 ± 3.9	1567 ± 26	6.9	5.0 ± 0.6
d	61.6 ± 2.5	11.3 ± 2.2	1884 ± 19	5.0	10.6 ± 1.4

approximately 7%. As the PEG is added, the elongations at break are substantially promoted, reaching 18.7% and 11.3% for CIM PLLA/PEG and OSIM PLLA/PEG, respectively. The tensile strength and Young's modulus rise from 64.9 and 1684 MPa for the CIM PLLA sample up to 73.7 and 1888 MPa for the OSIM PLLA one, respectively. More significant increase exists in the PLLA/PEG systems, the tensile strength and Young's modulus achieve 61.6 and 1884 MPa for OSIM PLLA/PEG, whereas it is only 48.9 and 1567 MPa for CIM PLLA/PEG, respectively. Furthermore, using the area under the stress−strain curve as list in Table 1, we can acquire information on the toughness or the energy absorbed by the bulk before breaking. The toughness of PLLA/PEG samples dramatically rises, compared with CIM PLLA sample, to a fairly high level with an increment of 228% for CIM PLLA/PEG and 164% for OSIM PLLA/PEG, achieving 6.9 and 5.0 MJ/m^3, respectively. The impact strength is also listed in Table 1, the OSIM PLLA/PEG specimen shows an outstanding performance in notched impact resistance with the impact strength of 10.6 KJ/m^2, which outperforms twice compared to those of other three specimens (approximately 4.5 KJ/m^2).

DMA was performed to acquire information on the thermal mechanical properties and mobility of chain segments. Figure 11 depicts the storage modulus (E'), loss modulus (E''), and damping parameter ($\tan\delta$) as a function of temperature. Effects of shish-kebab superstructure on PLLA stiffness at room temperature can be obviously seen in the inset table in Figure 11. An increase in E' of about 440 MPa at 25 °C is obtained for both OSIM samples compared to the corresponding CIM ones, which could be explained by the suppressed deformation by the introduction of shish-kebabs with preferentially oriented chains. The addition of PEG can result in a decrease of approximately 230 MPa in E' at 25 °C for both CIM and OSIM samples because of effective plasticization, but note that the E' of OSIM plasticized specimen is still even higher than that of CIM PLLA specimen, which indicates that formation of shish-kebabs can effectively overcome the softening effect of PEG on modulus of PLLA products. Additionally, PEG presents significant influence on the E' at higher temperature. During the heating round, the E' curves of CIM PLLA and OSIM PLLA show a moderate increase since 90 °C and present small peaks at around 95 °C. This is probably ascribed to the elevated crystallinity due to cold crystallization, which is observed in our previous work.[66] For PLLA/PEG samples, with the presence of fairly high crystallinity, no trace of cold crystallization is found. The plots of E'' versus temperature presented in Figure 11B are useful for detecting molecular mobility transitions, and the peak of E'' is interpreted as the T_g.[67] It is clear that OSIM samples containing shish-kebabs, compared to CIM ones, show a moderate increment of 1.5 °C in T_g, this is because that shish-kebabs can confine chain (segment) mobility in amorphous region. On the other hand, T_g of plasticized PLLA is reduced by ~5.4 °C, because of the considerable improved mobility of chain segments with the presence of PEG miscible with PLLA.[48] The tan δ values are in good agreement with the E'' data as shown in Figure 11C. The tan δ peaks are reduced in intensity for the OSIM samples and the CIM PLLA/PEG sample than that of CIM PLLA sample, resulting from the same suppressed effect of shish-kebabs or spherulite on the mobility of PLLA chains in amorphous region.

On the basis of previous efforts to overcome the intrinsic brittleness of PLLA parts, recent attempts to improve the mechanical properties of PLLA through addition of miscible or

dx.doi.org/10.1021/am3019756 | ACS Appl. Mater. Interfaces 2012, 4, 6774−6784

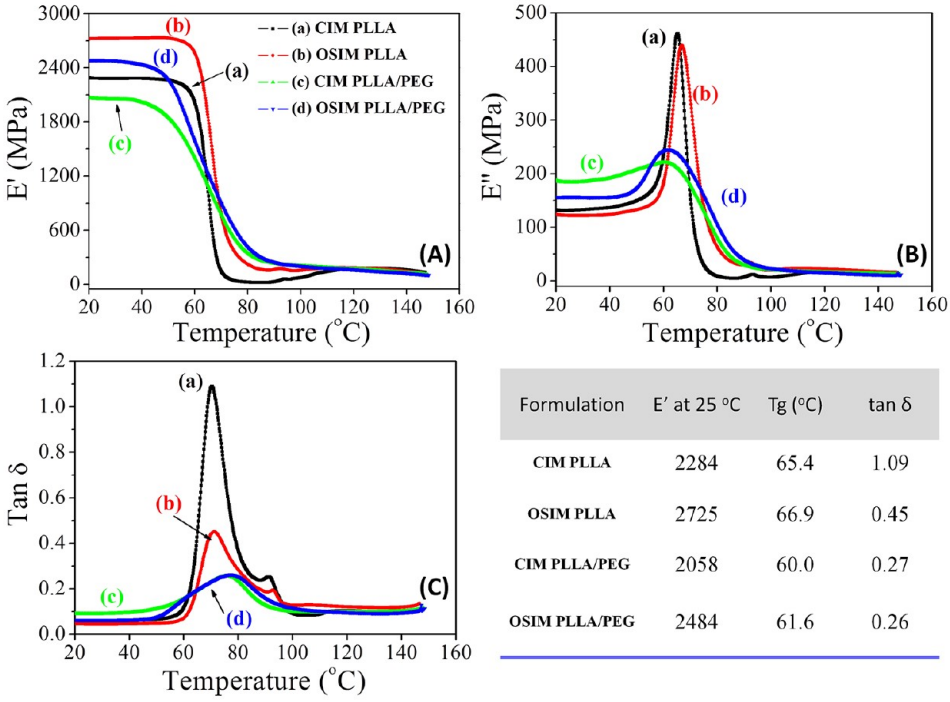

Formulation	E′ at 25 °C	Tg (°C)	tan δ
CIM PLLA	2284	65.4	1.09
OSIM PLLA	2725	66.9	0.45
CIM PLLA/PEG	2058	60.0	0.27
OSIM PLLA/PEG	2484	61.6	0.26

Figure 11. Temperature dependence of (A) storage modulus (E'), (B) loss modulus (E''), and (C) damping parameter (tan δ) for injection-molded pure PLLA and PLLA/PEG. The inset table summarizes the DMA results in detail.

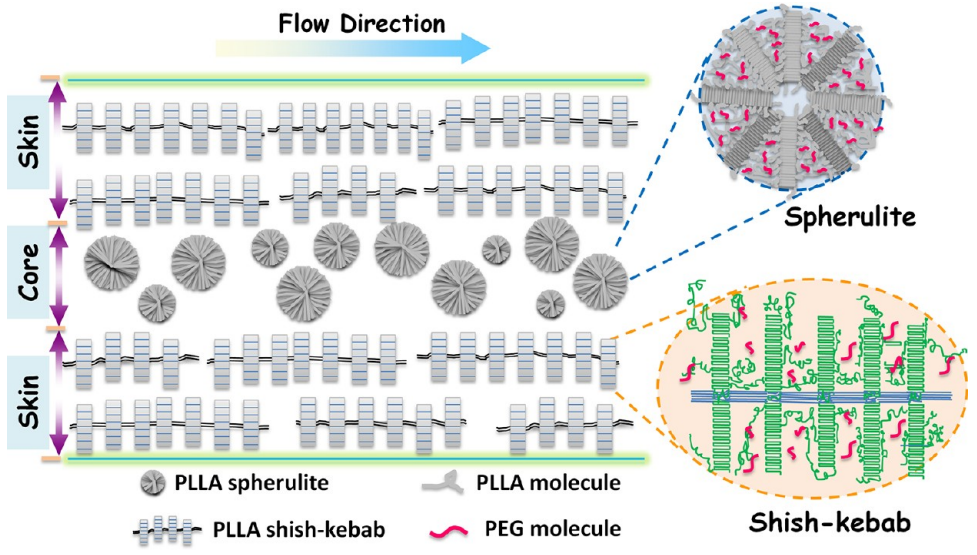

Figure 12. Schematic representation of bamboo-like structure in injection-molded PLLA/PEG induced by the combination of strong shear flow and PEG.

immiscible modifiers have been proved unsuccessful to some extent, primarily because of dramatically decreased strength and modulus, as well as limited improved impact strength.[7,51,68−71] For example, addition of 10 wt % PEG into PLLA pushed the tensile strength and modulus down to 26 and 900 MPa, respectively, and the modified PLLA with 20 wt % PEG almost lost its essential strength and modulus for general use.[52] In our case, the idea of developing shish-kebab superstructure through strong shear flow during practical processing successfully in this work overcomes these disadvantages effectively, leading to considerably simultaneous improvement of stiffness and ductility. A desirable balance of reinforcement and toughness of injection-molded PLLA parts has been achieved by the coexistence of shish-kebab superstructure and PEG. It is reasonably expected that our results obtained above will shed light on relaunching modification work for PLLA, i.e., achieving shish-kebab superstructure can reach a desirable balance of toughness, stiffness, and tensile strength.

Mechanism for Reinforcement and Toughening of PLLA by Formation of Shish-Kebabs. On the basis of structural similarity, we believe that all the polymeric materials containing shish-kebab superstructure probably share the same reinforcement and toughening mechanism, i.e., the shish structure with more extended chain conformation could act

as tight nanofibrils, permitting to effectively reinforce the polymer matrix in its own right.[44] More importantly, our exploration suggests a promising routine to toughen PLLA with a better balance of mechanical properties, i.e., a superior PLLA with excellent strength, modulus, ductility and toughness can be obtained under combined efforts of shear flow and PEG and the reinforcing and toughening mechanism in PLLA/PEG is specifically discussed below.

Figure 12 illustrates the structural schematic of PLLA/PEG formed during OSIM processing. As a whole, injection-molded PLLA sample containing PEG comprises two regions (i.e., outer layers and core layer), which have strikingly different crystalline morphology. Subjected to continuous, strong shear flow in outer layers (from the surface to intermediate layer), PLLA chains are prone to stretch and orient in the flow direction, therefore numerous fibrillar shish-kebabs with entended chains form a rather strong and hard outer layers. In the core region with relatively weak shear, PLLA chains get the chance to relax to coiled state and subsequently grow into spherulites, and PEG, located in the PLLA amorphous, is able to enhance mobility of chain segments and slippage of lamallae, therefore a "soft" core layer is reasonably expected. This hierachical strucuture is reminiscent of some natural creatures, such as bones and bamboos. They share the unique structure that contains soft material inside and tough shell outside as natural process of cross-disciplinary inspiration, leading to excellent antibending and antibreaking properties in an energetically favorable manner. Following this point of view, we could understand the hierarchical structure and mechanical performance relationship in the injetion-molded PLLA/PEG. With such a bamboo-like bionic structure, the material not only shows desirable properties of strength, modulus and ductility, but also presents great resistance to a sudden impact loading for that the tough "core" and hard "shell" are prone to absorb much energy and restrain crack propagation. That is to say, growing cracks are arrested in the fibrillar shish-kebabs and catastrophic failure is postponed in the loose core. The further understanding of this unique structure formed herein would fuel theoretical and technological interests in tailoring performance of PLLA at molecular level according to various requirements.

CONCLUSIONS

In this work, numerous shish-kebabs were successfully achieved in injection-molded parts of PLLA and PLLA/PEG systems, for the first time, by applying an intense shear flow field, which was provided by a modified injection molding technology of OSIM. This superstructure was not only clearly revealed by high-resolution SEM observations, but also further confirmed by typical SAXS patterns, showing a regular lamellae structure with cylindrical symmetry and a principal long period of 20 nm. Deducing from the high similarity in morphology and scattering patterns with those shish-kebabs of polyethylene and polypropylene obtained in flow field, we believe that the formation of PLLA shish-kebabs share the same mechanisms as the cases of polyethylene and polypropylene, but it appears that the critical conditions of PLLA shish-kebabs are more difficult to be fulfilled because of a semirigid chain backbone and relative low molecular weight, and it is hard to stretch and orient their chains to produce stable precursors and bundles of chain segments in the way like polyolefins. Furthermore, microbeam WAXD results revealed that PLLA crystal may presents α'-form due to its poor crystallization ability and rapid cooling during injection molding, whereas it transformed to α-form crystal once subjected to strong shear flow or the presence of PEG, both of which can substantially improve the crystallization kinetics of PLLA. With regard to mechanical properties, shish-kebabs of PLLA showed an obvious self-reinforced improvement in strength and stiffness. Structurally, the formation of self-reinforced shish-kebabs in PLLA/PEG system can gain an excellent balance of toughness, ductility and tensile properties, and the main reason may lie in the existing bamboo-like bionic structure that comprised hard skin of tight and fibrillar shish-kebabs as well as tough core consisting random amorphous PLLA (and PEG) chains and spherulites.

Our work could provide a promising doorway to achieve PLLA products with a desirable balance of various mechanical properties in the light of manipulating PLLA crystalline morphology. Instructively and significantly, an external strong shear flow and an addition of PEG hold great convenience and effectiveness in controlling the crystal structure and crystallization kinetics for PLLA. It is firmly believed that further exploration may give a rich fundamental understanding in the shear-induced crystallization and morphology manipulation of semirigid polymers.

AUTHOR INFORMATION

Corresponding Author

*Phone: +86-28-8540-0211 (G.-J.Z.); +86-28-8540-6866 (Z.-M.L.). Fax: +86-28-8540-6866 (G.-J.Z.); +86-28-8540-6866 (Z.-M.L.). E-mail: ganji.zhong@scu.edu.cn (G.-J.Z.); zmli@scu.edu.cn (Z.-M.L.).

Notes

The authors declare no competing financial interest.

ACKNOWLEDGMENTS

Special thanks must go to the National Natural Science Foundation of China (Grants 51120135002, 51121001, 51203104, and 50925311), and Startup Fund of Sichuan University (Grant 2011SCU11072) for financial support for this project. This work was also partially supported by Open Research Fund of State Key Laboratory of Polymer Physics and Chemistry, Changchun Institute of Applied Chemistry, Chinese Academy of Sciences (Grant 201014). We also would like to express sincere thanks to the Shanghai Synchrotron Radiation Facility (SSRF, Shanghai, China), for the kind help on 2D-WAXD and 2D-SAXS measurements.

REFERENCES

(1) Dorgan, J. R., Braun, B., Wegner, J. R., Knauss, D. M. Poly(lactic acids): A brief review. In *Degradable Polymers and Materials. Principles and Practice*; Khemani, K., Scholz, C., Eds.; American Chemical Society: Washington, D.C., 2006; pp 102−125.

(2) Gupta, B.; Revagade, N.; Hilborn, J. *Prog. Polym. Sci.* **2007**, *32*, 455−482.

(3) Lim, L. T.; Auras, R.; Rubino, M. *Prog. Polym. Sci.* **2008**, *33*, 820−852.

(4) Furukawa, T.; Matsusue, Y.; Yasunaga, T.; Shikinami, Y.; Okuno, M.; Nakamura, T. *Biomaterials* **2000**, *21*, 889−898.

(5) Shikinami, Y.; Okuno, M. *Biomaterials* **2001**, *22*, 3197−3211.

(6) Cai, X.; Tong, H.; Shen, X.; Chen, W.; Yan, J.; Hu, J. *Acta Biomater.* **2009**, *5*, 2693−2703.

(7) Lu, J.; Qiu, Z.; Yang, W. *Polymer* **2007**, *48*, 4196−4204.

(8) Rathi, S.; Chen, X.; Coughlin, E. B.; Hsu, S. L.; Golub, C. S.; Tzivanis, M. J. *Polymer* **2011**, *52*, 4184−4188.

(9) Gao, C.; Yu, L.; Liu, H.; Chen, L. *Prog. Polym. Sci.* **2012**, *37*, 767−780.

(10) Manninen, M. J.; Pohjonen, T. *Biomaterials* **1993**, *14*, 305−312.
(11) Kmetty, Á.; Bárány, T.; Karger-Kocsis, J. *Prog. Polym. Sci.* **2010**, *35*, 1288−1310.
(12) Furuhashi, Y.; Kimura, Y.; Yoshie, N.; Yamane, H. *Polymer* **2006**, *47*, 5965−5972.
(13) Shao, S.; Zhou, S.; Li, L.; Li, J.; Luo, C.; Wang, J.; Li, X.; Weng, J. *Biomaterials* **2011**, *32*, 2821−2833.
(14) Ferguson, S.; Wahl, D.; Gogolewski, S. *J. Biomed. Mater. Res., Part A* **1996**, *30*, 543−551.
(15) Binsbergen, F. L. *Nature* **1966**, *211*, 516−517.
(16) Bashir, Z.; Odell, J. A.; Keller, A. *J. Mater. Sci.* **1986**, *21*, 3993−4002.
(17) Somani, R. H.; Hsiao, B. S.; Nogales, A. *Macromolecules* **2001**, *34*, 5902−5909.
(18) Bent, J.; Hutchings, L. R.; Richards, R. W.; Gough, T.; Spares, R.; Coates, P. D.; Grillo, I.; Harlen, O. G.; Read, D. J.; Graham, R. S.; Likhtman, A. E.; Groves, D. J.; Nicholson, T. M.; McLeish, T. C. B. *Science* **2003**, *301*, 1691−1695.
(19) Kimata, S.; Sakurai, T.; Nozue, Y.; Kasahara, T.; Yamaguchi, N.; Karino, T.; Shibayama, M.; Kornfield, J. A. *Science* **2007**, *316*, 1014−1017.
(20) Housmans, J.-W.; Steenbakkers, R. J. A.; Roozemond, P. C.; Peters, G. W. M.; Meijer, H. E. H. *Macromolecules* **2009**, *42*, 5728−5740.
(21) Shen, B.; Liang, Y.; Zhang, C.; Han, C. C. *Macromolecules* **2011**, *44*, 6919−6927.
(22) Pennings, A. J.; Kiel, A. M. *Kolloid Z. Z. Polym.* **1965**, *205*, 160−162.
(23) Kumaraswamy, G.; Issaian, A. M.; Kornfield, J. A. *Macromolecules* **1999**, *32*, 7537−7547.
(24) Yang, L.; Somani, R. H.; Sics, I.; Hsiao, B. S.; Kolb, R.; Fruitwala, H.; Ong, C. *Macromolecules* **2004**, *37*, 4845−4859.
(25) Fukushima, H.; Ogino, Y.; Matsuba, G.; Nishida, K.; Kanaya, T. *Polymer* **2005**, *46*, 1878−1885.
(26) Hsiao, B. S.; Yang, L.; Somani, R. H.; Avila-Orta, C. A.; Zhu, L. *Phys. Rev. Lett.* **2005**, *94*, 117802.
(27) Byelov, D.; Panine, P.; de Jeu, W. H. *Macromolecules* **2007**, *40*, 288−289.
(28) Balzano, L.; Kukalyekar, N.; Rastogi, S.; Peters, G. W.; Chadwick, J. *Phys. Rev. Lett.* **2008**, *100*, 048302.
(29) Mykhaylyk, O. O.; Chambon, P.; Graham, R. S.; Fairclough, J. P. A.; Olmsted, P. D.; Ryan, A. J. *Macromolecules* **2008**, *41*, 1901−1904.
(30) Balzano, L.; Rastogi, S.; Peters, G. W. M. *Macromolecules* **2009**, *42*, 2088−2092.
(31) Cavallo, D.; Azzurri, F.; Balzano, L.; Funari, S. S.; Alfonso, G. C. *Macromolecules* **2010**, *43*, 9394−9400.
(32) Murase, H.; Ohta, Y.; Hashimoto, T. *Macromolecules* **2011**, *44*, 7335−7350.
(33) Somani, R. H.; Yang, L.; Zhu, L.; Hsiao, B. S. *Polymer* **2005**, *46*, 8587−8623.
(34) Wang, K.; Chen, F.; Zhang, Q.; Fu, Q. *Polymer* **2008**, *49*, 4745−4755.
(35) Bashir, Z.; Odell, J. A.; A., K. *J. Mater. Sci.* **1984**, *19*, 3713−3725.
(36) Matsuba, G.; Sakamoto, S.; Ogino, Y.; Nishida, K.; Kanaya, T. *Macromolecules* **2007**, *40*, 7270−7275.
(37) Somani, R. H.; Hsiao, B. S.; Nogales, A.; Srinivas, S.; Tsou, A. H.; Sics, I.; Balta-Calleja, F. J.; Ezquerra, T. A. *Macromolecules* **2000**, *33*, 9385−9394.
(38) Mykhaylyk, O. O.; Fernyhough, C. M.; Okura, M.; Fairclough, J. P. A.; Ryan, A. J.; Graham, R. *Eur. Polym. J.* **2011**, *47*, 447−464.
(39) Yan, T.; Zhao, B.; Cong, Y.; Fang, Y.; Cheng, S.; Li, L.; Pan, G.; Wang, Z.; Li, X.; Bian, F. *Macromolecules* **2010**, *43*, 602−605.
(40) Zhang, R.-C.; Xu, Y.; Lu, A.; Cheng, K.; Huang, Y.; Li, Z.-M. *Polymer* **2008**, *49*, 2604−2613.
(41) Yamazaki, S.; Itoh, M.; Oka, T.; Kimura, K. *Eur. Polym. J.* **2010**, *46*, 58−68.
(42) Li, X.-J.; Zhong, G.-J.; Li, Z.-M. *Chinese J. Polym. Sci.* **2010**, *28*, 357−366.
(43) Cao, W.; Wang, K.; Zhang, Q.; Du, R.; Fu, Q. *Polymer* **2006**, *47*, 6857−6867.
(44) Chen, Y.-H.; Zhong, G.-J.; Wang, Y.; Li, Z.-M.; Li, L. *Macromolecules* **2009**, *42*, 4343−4348.
(45) Zhong, G.-J.; Li, L.; Mendes, E.; Byelov, D.; Fu, Q.; Li, Z.-M. *Macromolecules* **2006**, *39*, 6771−6775.
(46) Li, S.-N.; Li, B.; Li, Z.-M.; Fu, Q.; Shen, K.-Z. *Polymer* **2006**, *47*, 4497−4500.
(47) Kulinski, Z.; Piorkowska, E. *Polymer* **2005**, *46*, 10290−10300.
(48) Pillin, I.; Montrelay, N.; Grohens, Y. *Polymer* **2006**, *47*, 4676−4682.
(49) Xu, L.; Chen, C.; Zhong, G.-J.; Lei, J.; Xu, J.-Z.; Hsiao, B. S.; Li, Z.-M. *ACS Appl. Mater. Interfaces* **2012**, *4*, 1521−1529.
(50) Kalay, G.; Kalay, C. R. *J. Polym. Sci. Polym. Phys.* **2002**, *40*, 1828−1834.
(51) Martin, O.; Avérous, L. *Polymer* **2001**, *42*, 6209−6219.
(52) Hu, Y.; Hu, Y. S.; Topolkaraev, V.; Hiltner, A.; Baer, E. *Polymer* **2003**, *44*, 5711−5720.
(53) Huang, S.; Li, H.; Jiang, S.; Chen, X.; An, L. *Polymer* **2011**, *52*, 3478−3487.
(54) Tsai, C.-C.; Wu, R.-J.; Cheng, H.-Y.; Li, S.-C.; Siao, Y.-Y.; Kong, D.-C.; Jang, G.-W. *Polym. Degrad. Stab.* **2010**, *95*, 1292−1298.
(55) Mahendrasingama, A.; Blundella, D. J.; Partona, M.; Wrighta, A. K.; Rasburnb, J.; Narayananc, T.; Fullera, W. *Polymer* **2005**, *46*, 6009−6015.
(56) Zhang, C.; Hu, H.; Wang, D.; Yan, S.; Han, C. C. *Polymer* **2005**, *46*, 8157−8161.
(57) Chakrabarti, D.; Jose, P.; Chakrabarty, S.; Bagchi, B. *Phys. Rev. Lett.* **2005**, *95*, 197801.
(58) Huang, M.-J.; Leonard, A. *Phys. Fluids* **1994**, *6*, 3765−3775.
(59) Tian, N.; Zhou, W.; Cui, K.; Liu, Y.; Fang, Y.; Wang, X.; Liu, L.; Li, L. *Macromolecules* **2011**, *44*, 7704−7712.
(60) Shinohara, Y.; Yamazoe, K.; Sakurai, T.; Kimata, S.; Maruyama, T.; Amemiya, Y. *Macromolecules* **2012**, *45*, 1398−1407.
(61) Schroer, C. G.; Kuhlmann, M.; Roth, S. V.; Gehrke, R. *Appl. Phys. Lett.* **2006**, *88*, 164102.
(62) Zhang, J.; Duan, Y.; Sato, H.; Tsuji, H.; Noda, I.; Yan, S.; Ozaki, Y. *Macromolecules* **2005**, *38*, 8012−8021.
(63) Gutiérrez, M. C. G.; Alfonso, G. C.; Riekel, C.; Azzurri, F. *Macromolecules* **2004**, *37*, 478−485.
(64) Kalay, G.; Sousa, R. A.; Reis, R. L.; Cunha, M.; Bevis, M. J. *J. Appl. Polym. Sci.* **1999**, *73*, 2473−2483.
(65) Liang, S.; Yang, H.; Wang, K.; Zhang, Q.; Du, R.; Fu, Q. *Acta Mater.* **2008**, *56*, 50−59.
(66) Xu, H.; Liu, C.-Y.; Chen, C.; Hsiao, B. S.; Zhong, G.-J.; Li, Z.-M. *Biopolymers* **2012**, *97*, 825−839.
(67) Idicula, M.; Malhotra, S. K.; Joseph, K.; Thomas, S. *Compos. Sci. Technol.* **2005**, *65*, 1077−1087.
(68) Gajria, A. M.; Dave, V.; Gross, R. A.; McCarthy, S. P. *Polymer* **1996**, *37*, 437−444.
(69) Ljungberg, N.; Wesslén, B. *Polymer* **2003**, *44*, 7679−7688.
(70) Ljungberg, N.; Wesslén, B. *Biomacromolecules* **2005**, *6*, 1789−1796.
(71) Ali, F.; Chang, Y.-W.; Kang, S. C.; Yoon, J. Y. *Polym. Bull.* **2009**, *62*, 91−98.